Polymer
Chemistry

Accepted Manuscript

ROYAL SOCIETY
OF CHEMISTRY

www.rsc.org/polymers

Journal Name

ARTICLE

Synthesis of Platinum-Containing Poly(phenyleneethynylene)s Having Various Chromophores. Aggregation and Optical Properties

Yu Miyagi,[a] Yuno Shibutani,[a] Yoshinori Otaki[a] and Fumio Sanda*[a]

The Sonogashira-Hagihara coupling polymerization of platinum-containing *m,m*-phenylene and *p,p*-phenylene-linked diethynyl monomers ***m,m*-1** and ***p,p*-1** with 1,4-dibromobenzene **2a**, 1,4-dibromonaphthalene **2b** and 9,10-dibromoanthracene **2c** was carried out to obtain the corresponding platinum-containing polymers [poly(***m,m*-1-2a**)–poly(***m,m*-1-2c**)] and [poly(***p,p*-1-2a**)–poly(***p,p*-1-2c**)] with M_n's ranging from 4,300 to 28,000 in 24%–quantitative yields. The UV-vis absorption and emission properties of the formed polymers were measured in various solvents to examine the solvent effect on the optical properties. These polymers emitted fluorescence at 400–600 nm with 3.4–18.0% quantum yields in THF, $CHCl_3$ and CH_2Cl_2. The fluorescence intensities of the polymers remarkably decreased upon raising MeOH concentration in THF/MeOH mixtures, accompanying the formation of aggregates.

Received 00th January 20xx,
Accepted 00th January 20xx

DOI: 10.1039/x0xx00000x

www.rsc.org/

INTRODUCTION

Conjugated polymers have attracted much attention due to their potentials for a broad range of photoelectrical applications,[1] including polyelectrolytes,[2] light-emitting diodes,[2] photovoltaic materials[3] and bio/chemo sensors.[4] Poly(phenyleneethynylene) is one of the most widely studied conjugated polymers. A wide variety of poly(phenyleneethynylene) derivatives, and cyclic/hyperbranched phenyleneethynylene derivatives have been synthesized to construct molecules with regulated geometries, folded and globular structures, and application to photoelectrically functional materials.[5] The conjugation length of poly(phenyleneethynylene)s is controllable by replacing the phenylene linkage with the other arylenes like naphthalene, anthracene, tetracene, pentacene etc., leading to tuning of photoelectric properties, especially UV-vis absorption and fluorescence emission.

Incorporation of metals in the main chain is another approach to control the structures and properties of poly(phenyleneethynylene)s. Various platinum (Pt) acetylide π-conjugated polymers and oligomers have been developed since the first report by Sonogashira et al.[6] Pt acetylide π-conjugated systems transport energy through the conjugated main chain,[7] and find applications in nonlinear optical materials and photovoltaic devices. Schanze and coworkers reported the formation of a triplet exciton in a Pt acetylide chromophore system.[7b,8] Although there are many reports on Pt-containing poly(aryleneethynylene)s as well as the secondary structures of conjugated polymers including poly(acetylene)s,[9] poly(aniline)s[10], poly(phenylene)s[11] poly(phenylenevinylene)s[12] and poly(phenyleneethynylene)s,[13] there are few reports concerning the effect of aggregation on the photophysical properties of Pt acetylide conjugated polymers.[14] We reported the synthesis and examination of the secondary structures of various poly(aryleneethynylene)s, some of which formed folded helices and/or aggregates depending on temperature and polarity of solvent.[15] We recently synthesized optically active poly(aryleneethynylene)s containing Pt in the main chain by the Sonogashira-Hagihara coupling polymerization of D-hydroxyphenylglycine-derived optically active diiodoareylene monomers with a Pt-containing diethynyl monomer to find that amide-substituted polymers formed chiral aggregates in polar media (THF/MeOH mixtures), while they formed one-handed helices in nonpolar media (THF/toluene mixtures).[16] In the course of our study on Pt-containing poly(aryleneethynylene)s, we decided to examine the aggregation behavior of the polymers in more detail. In this paper, we report the synthesis of a series of *m,m*- and *p,p*-linked poly(phenyleneethynylene aryleneethynylene)s bearing Pt in the main chain and investigation of the relationship between the optical and aggregation properties.

---

[a] *Department of Chemistry and Materials Engineering, Faculty of Chemistry, Materials and Bioengineering, Kansai University, 3-3-35 Yamate-cho, Suita, Osaka 564-8680, Japan. E-mail: sanda@kansai-u.ac.jp*

† Electronic Supplementary Information (ESI) available: Structures and band gaps of model compounds for polymers with and without platinum (Fig. S1, Table S1); Relationships between band gap of model compounds for polymers vs λ_{edge} of absorption of polymers and absorption maxima of polymers (Fig. S2); relative energy of aggregates of four model molecules, calculated by the DFT method [M06-2X/6-31G* (C, H, P)-LANL2DZ (Pt)]; ^1H, ^{13}C, ^{31}P NMR and IR spectra of the monomer and polymers (Fig. S3–S9). See DOI: 10.1039/x0xx00000x

EXPERIMENTAL SECTION

Measurements.
^{1}H (400 MHz) and ^{13}C (100 MHz) NMR spectra were recorded on a JEOL EX-400 or a JEOL AL-400 spectrometer. IR spectra were acquired on a JASCO FT/IR-4100 spectrophotometer. Melting points (mp) were measured on a Yanaco micro melting point apparatus. Mass spectra were acquired on a Thermo Scientific Exactive mass spectrometer. Number- and weight-average molecular weights (M_n and M_w) of polymers were determined by SEC (columns: TSK gel α-M, GMHXL, Shodex KF-805L × 3; JASCO RI-930, JASCO UV-1570, JASCO PU-980, JASCO DG-980-50, CO-965) using tetrahydrofuran (THF) as the eluent with polystyrene standards at 40 °C. UV-vis absorption spectra were recorded on a JASCO V-550 spectropolarimeter. Fluorescence spectra were obtained on a JASCO FP-750 and a HITACHI F-7000 spectrophotometers. DLS measurements were performed using a Malvern Instruments Zetasizer Nano ZS at 25 °C. The measured autocorrelation function was analyzed using a cumulant method. The *Z*-average values of the polymers were calculated from the Stokes-Einstein equations.

Materials.
trans-Bis(4-ethynylphenylethynyl)-bis(tributylphosphine)Pt(II)[17] (5) and [PdCl$_2$(PPh$_3$)$_2$][18] were synthesized according to the literature. Reagents including [Pd(PPh$_3$)$_4$] (Aldrich, assay 99.9%) and CuI (Wako, 99.5%) were used as received. Solvents used for polymerization were dried with the molecular sieves 4A 1/16 and degassed using the freeze-pump-thaw method.

Monomer Synthesis.
1-Bromo-3-[2-(trimethylsilyl)ethynyl]benzene. [PdCl$_2$(PPh$_3$)$_2$] (1.05 g, 1.49 mmol), PPh$_3$ (0.391 g, 1.49 mmol), CuI (0.284 g, 1.49 mmol) and trimethylsilylacetylene (TMSA, 7.11 mL, 50 mmol) were added to a solution of 1-bromo-3-iodobenzene (14.14 g, 50 mmol) in THF/Et$_3$N (15 mL/30 mL) under argon at 0 °C, and the resulting mixture was stirred at 45 °C overnight. After filtration, the filtrate was concentrated to obtain a black solid. The residual mass was purified by silica gel column chromatography eluted with CHCl$_3$/hexane = 1/1 (v/v) to obtain 1-bromo-3-[2-(trimethylsilyl)ethynyl]benzene as a yellow solid in 96% yield. ^{1}H NMR (400 MHz, CDCl$_3$): δ 0.24 (s, 9H, –Si(CH_3)$_3$), 7.14–7.18 (m, 1H, Ar), 7.37–7.39 (m, 1H, Ar), 7.42–7.45 (m, 1H, Ar), 7.61 (s, 1H, Ar).

2-Methyl-4-{3-[(trimethylsilyl)ethynyl]phenyl}-3-butyn-2-ol. [PdCl$_2$(PPh$_3$)$_2$] (1.05 g, 1.49 mmol), PPh$_3$ (0.63 g, 2.4 mmol), CuI (0.284 g, 1.49 mmol), 2-methyl-3-butyn-2-ol (5.16 mL, 52.8 mmol) were added to a solution of 1-bromo-3-[2-(trimethylsilyl)ethynyl]benzene (12.09 g, 48 mmol) in THF/Et$_3$N (25 mL/25 mL) under argon at 0 °C, and the resulting mixture was stirred with refluxing at 80 °C for 6 h. After filtration, the filtrate was concentrated to obtain a black solid. The residual mass was purified by silica gel column chromatography eluted with CHCl$_3$/hexane = 1/1–2/1 (v/v) to obtain 2-methyl-4-{3-[(trimethylsilyl)ethynyl]phenyl}-3-butyn-2-ol as a red solid in 86% yield. ^{1}H NMR (400 MHz, CDCl$_3$): δ 0.23 (s, 9H, –Si(CH_3)$_3$), 1.60 (s, 6H, –CH_3), 1.94 (s, 1H, –OH), 7.19–7.57 (m, 4H, Ar).

1-Ethynyl-3-[2-(trimethylsilyl)ethynyl]benzene. NaOH (1.65 g, 41.2 mmol) was added to a solution of 2-methyl-4-{3-[(trimethylsilyl)ethynyl]phenyl}-3-butyn-2-ol (10.55 g, 41.2 mmol) in toluene (135 mL) under argon at 0 °C, and the resulting mixture was stirred with refluxing at 110 °C for 0.5 h. After filtration, the filtrate was concentrated to obtain a black liquid. The residual mass was purified by silica gel column chromatography eluted with dichloromethane/hexane = 1/1 (v/v), followed by Kugelrohr distillation to obtain 2-methyl-4-{3-[(trimethylsilyl)ethynyl]phenyl}-3-butyn-2-ol as a yellow liquid in 49% yield. ^{1}H NMR (400 MHz, CDCl$_3$): δ 0.24 (s, 9H, –Si(CH_3)$_3$), 3.07 (m, 1H, –CH), 7.22–7.62 (m, 4H, Ar). ^{13}C NMR (100 MHz, CDCl$_3$): δ 0.02, 82.6, 82.7, 95.2, 103.9, 122.4, 123.5, 128.3, 128.5, 132.0, 132.2, 132.4, 135.5, 135.7.

Bis{3-[2-(trimethylsilyl)ethynyl]phenylethynyl}bis(butylphosphine)platinum. 1-Ethynyl-3-[2-(trimethylsilyl)ethynyl]benzene (0.46 g, 2.3 mmol), [PtCl$_2$(PBu$_3$)$_2$] (0.80 g, 1.2 mmol), CuI (0.044 g, 0.23 mmol) were dissolved in Et$_2$NH (34 mL) under argon at 0 °C, and the resulting mixture was stirred with refluxing at 65 °C for 4 h. After filtration, the filtrate was concentrated to obtain a purple solid. The residual mass was purified by silica gel column chromatography with dichloromethane/hexane = 4/1–2/1(v/v) as the eluent to obtain bis{3-[2-(trimethylsilyl)ethynyl]phenylethynyl}bis(butylphosphine)platinum as a yellow solid in 42% yield. ^{1}H NMR (400 MHz, CDCl$_3$): δ 0.24 (s, 9H, –Si(CH_3)$_3$), 0.92 (t, J = 5.2 Hz, 18H, –CH_3), 1.39–1.67 (m, 28H, –CH_2CH_2–), 2.04–2.22 (m, 12H, –CH_2–), 7.08–7.41 (m, 8H, Ar).

Bis[(3-ethynylphenyl)ethynyl]bis(butylphosphine)platinum (***m*,*m*-1**). KOH (0.28 g, 41.2 mmol) dissolved in water (5 mL) were added to a solution of bis{3-[2-(trimethylsilyl)ethynyl]phenylethynyl}bis(butylphosphine)platinum (0.50 g, 0.5 mmol) in THF/methanol (55 mL/40 mL) at 0 °C, and the resulting mixture was stirred at room temperature for 5 h. After filtration, the filtrate was concentrated to obtain a yellow liquid. The residual mass was purified by silica gel column chromatography with CHCl$_3$ as the eluent to obtain ***m*,*m*-1** as a yellow solid in 97% yield. Mp 85–86 °C. IR (KBr): 3433, 3277 (–$C{\equiv}C$–H), 2956, 2927, 2871, 2096 (–$C{\equiv}C$–Pt–), 1597, 1500, 1215, 1092, 835, 584 cm^{-1}. ^{1}H NMR (400 MHz, CDCl$_3$): δ 0.92 (t, J = 7.6 Hz, 18H, –CH_3), 1.38–1.65 (m, 24H, –CH_2CH_2–), 2.04–2.20 (m, 12H, –CH_2–), 7.11–7.39 (m, 8H, Ar). ^{13}C NMR (100 MHz, CDCl$_3$): δ 13.8, 24.4, 26.4, 83.8, 108.1, 109.7, 121.7, 128.0, 128.5, 129.2, 131.2,134.4. ^{31}P NMR (162 MHz, CDCl$_3$) δ 3.80 ($J_{\text{Pt–P}}$ = 2346 Hz, corresponding to a trans isomer[13]). MALDI-TOF-MS: *m/z* calcd for $C_{44}H_{64}P_2Pt$: 849.41; found 848.98. Anal.Calcd for $C_{44}H_{64}P_2Pt$: C, 62.17; H, 7.59. Found: C, 61.79; H, 7.64.

Bis[(4-ethynylphenyl)ethynyl]bis(butylphosphine)platinum (***p*,*p*-1**). This compound was synthesized according to the literature. Yield 85%. Mp 93–95 °C. IR (KBr): 3433, 3277 (–$C{\equiv}C$–H), 2956, 2927, 2871, 2096 (–$C\equiv C$–Pt–), 1597, 1500, 1215, 1092, 835, 584 cm^{-1}. ^{1}H NMR (400 MHz, $CDCl_3$): δ 0.89 (t, J = 7.4 Hz, 18H, –CH_3), 1.54 (s, 36H, –$CH_2CH_2CH_2$–), 3.07 (s, 2H, –CH), 7.16 (d, J = 8.0 Hz, 4H, Ar), 7.30 (d, J = 8.0 Hz, 4H, Ar). ^{31}P NMR (162 MHz, $CDCl_3$) δ 3.83 (J_{Pt-P} = 2346 Hz, corresponding to a trans isomer[19]).

Scheme 1 Synthesis of monomer ***m,m*-1**.

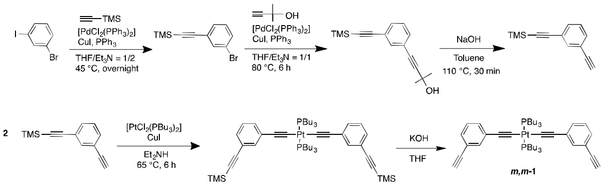

Polymerization.

All polymerizations were carried out in a glass tube equipped with a three-way stopcock under argon. In a typical experiment, a solution of $[Pd(PPh_3)_4]$ (2.89 mg, 2.5 μmol) in THF (0.4 mL) and a solution of CuI (0.47 mg, 2.5 μmol) in Et_3N (0.6 mL) were added to a mixture of monomers ***m,m*-1** or ***p,p*-1** (42.5 mg, 0.05 mmol) and **2a**–**2c** (0.05 mmol) under argon, and the resulting solution was kept at 60 °C for 24 h. Then, the reaction mixture was poured into a large volume of methanol to precipitate the polymer. It was separated by filtration using a membrane filter (ADVANTEC H100A047A) and dried under reduced pressure.

Spectroscopic Data of the Polymers. Poly(***p,p*-1-2a**): IR (KBr): 3448, 2958, 2927, 2871, 2097 (–$C\equiv C$–Pt–), 1513, 1457, 1256, 1097, 1024, 903, 835, 801, 722 cm^{-1}. ^{1}H NMR (400 MHz, $CDCl_3$): δ 0.92–0.94 (br, 18H, –CH_2CH_3), 1.43–1.53 [br, 24H, –$CH_2(CH_2)_3$–], 2.05–2.12 [br, 12H, –$CH_2(CH_2)_3$–] 7.10–7.76 (br, 12H, Ar). Poly(***m,m*-1-2a**): IR (KBr): 3448, 2931, 2871, 2738, 2802, 2738, 2678, 2492, 2097 (–$C\equiv C$–Pt–), 1587, 1433, 1399, 1383, 1262, 1206, 1170, 1095, 1036, 889, 836, 789, 721, 688 cm^{-1}. ^{1}H NMR (400 MHz, $CDCl_3$): δ 0.92-0.94 (br, 18H, –CH_2CH_3), 1.30–1.48 [br, 24H, –$CH_2(CH_2)_3$–], 2.05–2.13 [br, 12H, –$CH_2(CH_2)_3$–] 7.04–7.75 (br, 12H, Ar). Poly(***p,p*-1-2b**): IR (KBr): 3448, 2957, 2926, 2870, 2095 (–$C\equiv C$–Pt–), 1555, 1500, 1262, 1213, 1170, 1095, 904, 834, 801, 721, 669 cm^{-1}. ^{1}H NMR (400 MHz, CD_3OD): δ 0.92-0.94 (br, 18H, –CH_2CH_3), 1.35–1.63 [br, 24H, –$CH_2(CH_2)_3$–], 2.05–2.15 [br, 12H, –$CH_2(CH_2)_3$–] 6.84–8.47 (br, 14H, Ar). Poly(***m,m*-1-2b**): IR (KBr): 3434, 3057, 2961, 2928, 2871, 2096 (–$C\equiv C$–Pt–), 1587, 1474, 1406, 1379, 1341, 1262, 1093, 1024, 887, 864, 766, 687, 706, 661 cm^{-1}. ^{1}H NMR (400 MHz, $CDCl_3$): δ 0.91-0.94 (br, 18H, –CH_2CH_3), 1.40–1.64 [br, 24H, –$CH_2(CH_2)_3$–], 2.05–2.16 [br, 12H, –$CH_2(CH_2)_3$–] 7.05–8.47 (br, 14H, Ar). Poly(***p,p*-1-2c**): IR ($CHCl_3$ solution): 3448, 2958, 2927, 2871, 2096 (–$C\equiv C$–Pt–), 1595, 1559, 1503, 1262, 1213, 1173, 1095, 1026, 904, 833, 803, 766, 722 cm^{-1}. ^{1}H NMR (400 MHz, $CDCl_3$): δ 0.95-0.99 (br, 18H, –CH_2CH_3), 1.40–1.65 [br, 24H, –$CH_2(CH_2)_3$–], 2.12–2.25 [br, 12H, –$CH_2(CH_2)_3$–] 7.21–8.69 (br, 16H, Ar). Poly(***m,m*-1-2c**): IR (KBr): 3448, 3058, 2960, 2928, 2871, 2100 (–$C\equiv C$–Pt–), 1586, 1473, 1412, 1379, 1262, 1093, 1022, 887, 863, 803, 766, 687, 641 cm^{-1}. ^{1}H NMR (400 MHz, $CDCl_3$): δ 0.95-0.99 (br, 18H, –CH_2CH_3), 1.47–1.67 [br, 24H, –$CH_2(CH_2)_3$–], 2.10–2.25 [br, 12H, –$CH_2(CH_2)_3$–] 7.22–8.69 (br, 16H, Ar).

Computation.

All calculations were performed with the GAUSSIAN 09 program,[20] ES64L-G09 Rev D.01, running on the supercomputer system, Academic Center for Computing and Media Studies, Kyoto University. The energies were calculated by the density functional theory (DFT) with the B3LYP[21] or M06-2X[22] functional in conjunction with the 6-31G* or LANL2DZ basis set.

RESULTS AND DISCUSSION

Polymerization.

The Sonogashira-Hagihara coupling polymerization of bis[(ethynylphenyl)ethynyl]bis(butylphosphine) platinum monomers ***m,m*-1** and ***p,p*-1** with dibromoarylenes **2a**–**2c** was carried out using Pd-Cu catalyst (Scheme 2). First, the polymerization of ***m,m*-1** with **2a** was carried out using $[PdCl_2(PPh_3)_2]$-PPh_3 and CuI in THF/Et_3N = 2/3 at 60 °C for 24 h to obtain a polymer quantitatively (run 1 in Table 1), but the resultant polymer was insoluble in common organic solvents including $CHCl_3$, DMF and THF. When DMF was used as a solvent, the polymer yield decreased to 24% and the obtained polymer was still solvent-insoluble (run 2). On the other hand, the polymerization of ***m,m*-1** with **2a** using $[Pd(PPh_3)_4]$ and CuI in THF/Et_3N = 2/3 gave a THF-, $CHCl_3$- and CH_2Cl_2-soluble polymer with M_n = 12,000 in 87% yield (run 3). We therefore employed these conditions for the polymerization of the other combination of monomers (***m,m*-1** + **2b**, **2c**, ***p,p*-1** + **2a**–**2c**) to obtain the corresponding polymers quantitatively with M_n's ranging from 4,300 to 28,000 (runs 4–8). The IR and ^{1}H NMR spectra of the polymers were very consistent with the structures linked by Pt acetylide moieties (Fig. S4–S9).

Scheme 2 Sonogashira-Hagihara coupling polymerization of ***m,m*-1** and ***p,p*-1** with **2a**–**2c**.

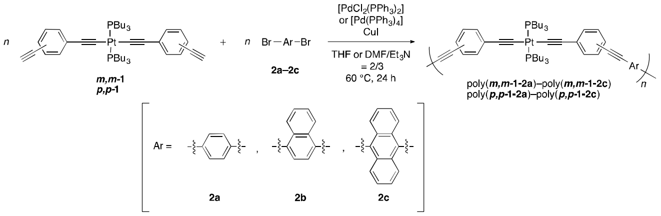

Table 1 Sonogashira-Hagihara coupling polymerization of ***m,m*-1** and ***p,p*-1** with **2a**–**2c**[a]

Run	Monomers	Catalyst	Solvent (v/v)	Yield[b] (%)	M_n[c]	M_w/M_n[c]
1	***m,m*-1** + **2a**	$[PdCl_2(PPh_3)_2]$, PPh_3, CuI	THF/Et_3N = 2/3	quant.	–	–
2	***m,m*-1** + **2a**	$[PdCl_2(PPh_3)_2]$, PPh_3, CuI	DMF/Et_3N = 2/3	24	–	–
3	***m,m*-1** + **2a**	$[Pd(PPh_3)_4]$, CuI	THF/Et_3N = 2/3	87	12,000	1.38
4	***m,m*-1** + **2b**	$[Pd(PPh_3)_4]$, CuI	THF/Et_3N = 2/3	quant.	7,100	2.08
5	***m,m*-1** + **2c**	$[Pd(PPh_3)_4]$, CuI	THF/Et_3N = 2/3	quant.	4,300	3.72
6	***p,p*-1** + **2a**	$[Pd(PPh_3)_4]$, CuI	THF/Et_3N = 2/3	quant.	11,600	3.00
7	***p,p*-1** + **2b**	$[Pd(PPh_3)_4]$, CuI	THF/Et_3N = 2/3	quant.	28,000	3.39
8	***p,p*-1** + **2c**	$[Pd(PPh_3)_4]$, CuI	THF/Et_3N = 2/3	quant.	20,400	4.41

---

[a] Conditions: [***m,m*-1**, ***p,p*-1**]$_0$ = [**2a–2c**] = 0.05 M, [***m,m*-1**, ***p,p*-1**]$_0$/[Pd] = 5, [Pd]/[CuI] = 1, 24 h under Ar. [b] MeOH-insoluble part. [c] Estimated by SEC eluted with THF, polystyrene calibration.

Optical Properties of the Polymers.

The UV-vis and emission spectra of the polymers obtained from runs 3–8 in Table 1 were measured in THF (Fig. 1 and 2). The λ_{max} values of the *m*-linked polymers [poly(***m,m*-1-2a**)–poly(***m,m*-1-2c**)] were shorter than those of the *p*-linked counterparts [poly(***p,p*-1-2a**)–poly(***p,p*-1-2c**)]. This result indicates that the conjugation length of the *m*-linked polymers were shorter than that of the corresponding *p*-linked compounds. The order of wavelength maxima of λ_{abs} and λ_{emi} of the *m*- and *p*-linked polymers was as follows: Ar = 1,4-phenylene < 1,4-naphthalene < 9,10-anthracene. This agrees with the order of the λ_{max} of the corresponding aromatics: benzene (255 nm) < naphthalene (286 nm) < anthracene (375 nm).[23] The number of fused aromatic rings apparently affected the absorption and emission properties of the polymers. The trend of λ_{max} of the polymers agreed well with that of the band gaps[24] of the model compounds (Fig. 3) for the polymers, which were calculated by the DFT method as listed in Table 2. [25]

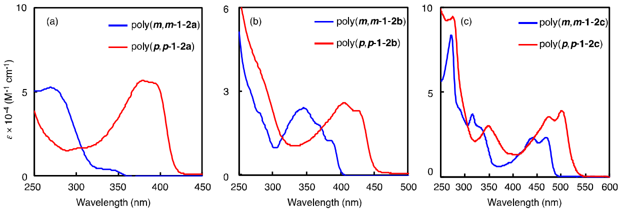

Fig. 1 UV-vis absorption spectra of (a) 1,4-phenylene-, (b) 1,4-naphthalene- and (c) 9,10-anthracene-based polymers measured in THF (*c* = 2 μM) at 20 °C.

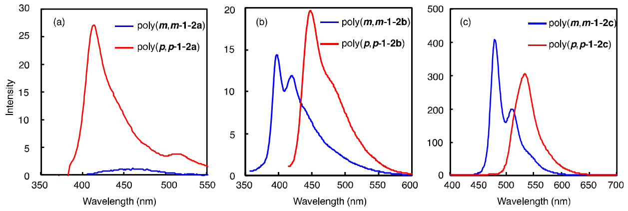

Fig. 2 Fluorescence spectra of (a) 1,4-phenylene, (b) 1,4-naphthalene- and (c) 9,10-anthracene-based polymers measured in THF (*c* = 2 μM) at 20 °C. Excitation wavelengths: poly(***m,m*-1-2a**), λ_{ex} = 269 nm; poly(***p,p*-1-2a**), λ_{ex} = 380 nm; poly(***m,m*-1-2b**), λ_{ex} = 345 nm; poly(***p,p*-1-2b**), λ_{ex} = 406 nm; poly(***m,m*-1-2c**), λ_{ex} = 440 nm; poly(***p,p*-1-2c**), λ_{ex} = 474 nm.

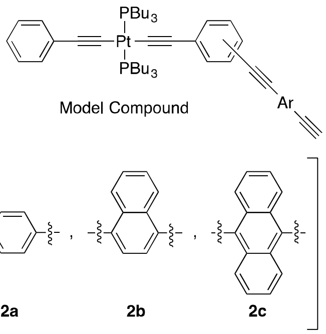

Fig. 3 Structures of the model compounds for the polymers.

Table 2 Band gaps of the model compounds for the polymers [a]

Polymer	HOMO (eV)	LUMO (eV)	Band gap (eV)
Poly(***m,m*-1-2a**)	-5.03	-1.41	3.62
Poly(***m,m*-1-2b**)	-5.02	-1.70	3.31
Poly(***m,m*-1-2c**)	-4.93	-2.13	2.80
Poly(***p,p*-1-2a**)	-4.88	-1.42	3.46
Poly(***p,p*-1-2b**)	-4.89	-1.73	3.16
Poly(***p,p*-1-2c**)	-4.74	-2.10	2.64

[a] Calculated for the model compounds by B3LYP/6-31G* (C, H, P)-LANL2DZ (Pt). The structures of the model compounds are illustrated in Fig. 3.

The UV-vis absorption and fluorescence spectra of poly(***m,m*-1-2c**) and poly(***p,p*-1-2c**) were measured in CH_2Cl_2 and $CHCl_3$ in addition to THF to check the solvent effect on the optical properties (Fig. 4 and 5).[26] The orders of the absorbances and emission intensities of poly(***m,m*-1-2c**) were CH_2Cl_2 ≈ $CHCl_3$ < THF and CH_2Cl_2 < THF ≈ $CHCl_3$, respectively. The absorbances of poly(***p,p*-1-2c**) were larger than those of poly(***m,m*-1-2c**) in the solvents. It is assumed that the degrees of aggregation are affected by solvents, bringing about the difference of the UV-vis absorbances and fluorescence emission intensities between the solvents. The aggregation of the polymers is discussed later in this manuscript.

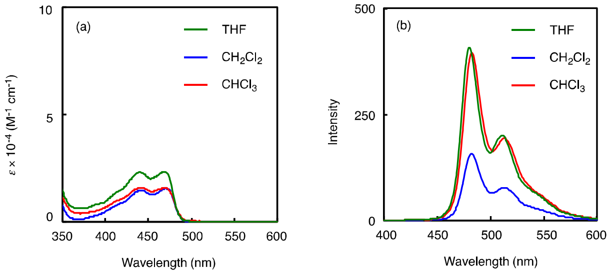

Fig. 4 (a) UV-vis absorption and (b) fluorescence spectra of poly(***m,m*-1-2c**) measured in THF, CH_2Cl_2 and $CHCl_3$ (*c* = 2 μM) at 20 °C. Excitation wavelength: 440 mm.

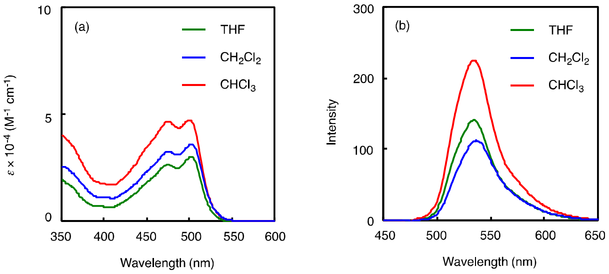

Fig. 5 (a) UV-vis absorption and (b) fluorescence spectra of poly(***p,p*-1-2c**) excited at 475 mm measured in THF, CH_2Cl_2 and $CHCl_3$ (c = 1 μM) at 20 °C.

The photoluminescence of Pt-containing polymers consists of a singlet emission and triplet emission.[7c,f] The present m-linked polymers emitted green fluorescence at 450–600 nm [Fig. 4 (b)] and p-linked polymers emitted yellow fluorescence at 500–650 nm [Fig. 5 (b)] assignable to singlet emission judging from the small Stokes shifts. It is likely that the polymers have relatively high band gaps based on the data of the model compounds (Table S1). Table 3 summarizes the absolute fluorescence quantum yields (φ) of poly(***m,m*-1-2c**) and poly(***p,p*-1-2c**) measured in THF, CH_2Cl_2 and $CHCl_3$. The φ values of poly(***m,m*-1-2c**) were larger than those of poly(***p,p*-1-2c**) regardless of solvent. It is likely that *m*-phenylene-linked poly(***m,m*-1-2c**) with a zigzag main chain is unfavorable for forming π-stacking-based aggregates compared with *p*-phenylene-linked poly(***p,p*-1-2c**) with a linear main chain. Consequently, poly(***m,m*-1-2c**) causes smaller aggregation-induced fluorescence quenching than poly(***p,p*-1-2c**). The φ value of poly(***p,p*-1-2c**) was larger in THF than those in CH_2Cl_2 and $CHCl_3$. It is considered that THF molecules coordinate to polymer molecules more strongly than CH_2Cl_2 and $CHCl_3$ molecules, resulting in segregation of polymer molecules. Although poly(***p,p*-1-2c**) emitted fluorescence more strongly in $CHCl_3$ than in THF as shown in Figure 5 (b), the φ was smaller in $CHCl_3$ (4.2%) than that in THF (14.4%). This is caused by the larger ε in $CHCl_3$ compared to that in THF as shown in Figure 5 (a).

Table 3 Absolute fluorescence quantum yields of poly(***m,m*-1-2c**) and poly(***p,p*-1-2c**)[a]

Polymer	Absolute fluorescence quantum yield (%)		
	in THF	in CH_2Cl_2	in $CHCl_3$
Poly(***m,m*-1-2c**)	18.0	3.5	24.0
Poly(***p,p*-1-2c**)	14.4	3.4	4.2

[a] c = 20 μM measured at 20 °C using an integrating sphere.

Aggregation of the polymers.

The optical properties of the polymers seem to be affected by aggregation, as mentioned above. Solutions of poly(***m,m*-1-2c**) and poly(***p,p*-1-2c**) in THF/MeOH mixtures were analyzed by DLS to obtain information on aggregation, wherein MeOH is a poor solvent for the polymers. The mean particle size of poly(***p,p*-1-2c**) tended to increase upon raising MeOH content as shown in Fig. 6. The formation of precipitates was observed and no reliable DLS data could be collected when MeOH content exceeded 40%. On the other hand, poly(***m,m*-1-2c**) did not show this trend regarding MeOH content[27] It is apparent that poly(***p,p*-1-2c**) forms aggregates more easily than poly(***m,m*-1-2c**). The UV-vis signals of the two polymers were somewhat affected by MeOH content but no clear tendency was observed, as shown in Fig. 7 (a) and 8 (a). On the contrary, the emission intensities apparently decreased by raising MeOH content, as shown in Fig. 7 (b) and 8 (b). The emission maximum of poly(***p,p*-1-2c**) appeared at around 530 nm when the MeOH content was 40% and less, while it appeared at around 550–560 nm when the MeOH content was 50% and more [Fig. 8 (b)]. This significant change is attributable to the formation of aggregates with large sizes, which were not appropriately determined by DLS measurement. It should be noted that poly(***m,m*-1-2c**) did not show such a critical point [Fig. 7 (b)], in agreement with the trend of particle size dependence on solvent composition. The solvent-dependence of UV-vis absorption λ_{max}, (b) ε_{max} and (c) emission intensity max are summarized in Fig. 9.

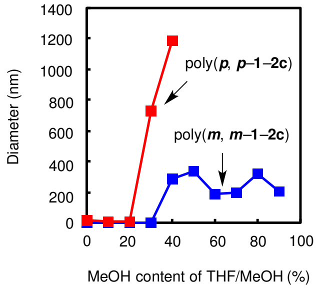

Fig. 6 Mean particle sizes of poly(***m,m*-1-2c**) and poly(***p,p*-1-2c**) (c = 20 μM) measured by DLS in THF/MeOH mixtures with various compositions at 20 °C.

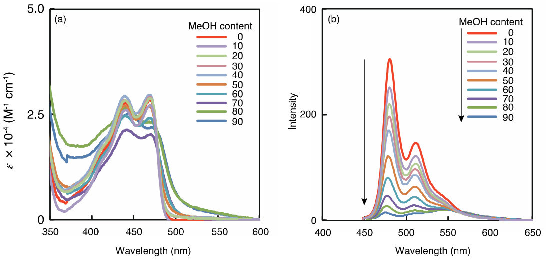

Fig. 7 (a) UV-vis absorption and (b) fluorescence spectra of poly(***m,m*-1-2c**) (c = 1 μM) excited at 439–443 nm measured in THF/MeOH mixtures with various compositions at 20 °C.

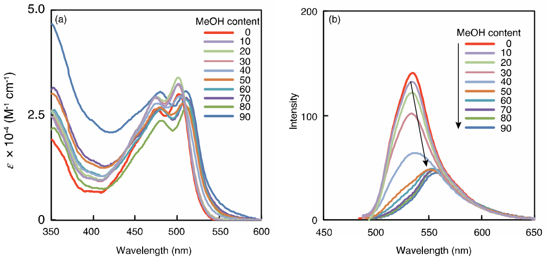

Fig. 8 (a) UV-vis absorption spectra and (b) fluorescence spectra of poly(***p,p*-1-2c**) (c = 1 µM) excited at 474–480 nm measured in THF/MeOH mixtures with various compositions at 20 °C.

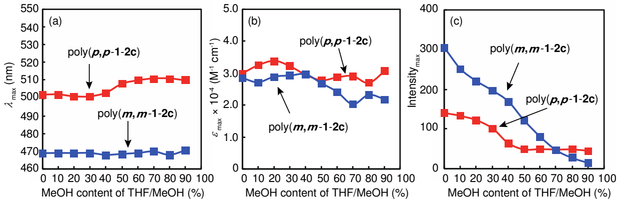

Fig. 9 (a) UV-vis absorption λ_{max}, (b) ε_{max} and (c) emission intensity max of poly(***m,m*-1-2c**) and poly(***p,p*-1-2c**) (c = 1 µM) measured in THF/MeOH mixtures with various compositions at 20 °C. Excited wavelength: poly(***m,m*-1-2c**), λ_{ex} = 340 nm; poly(***p,p*-1-2c**), λ_{ex} = 374 nm.

Possible aggregated structures

Molecular modeling was carried out to obtain information about the polymer aggregation process. As studied by Schanze and coworkers, Pt-acetylide oligomers [(–≡–Pt(PR$_3$)$_2$–≡–Ar–)$_n$] possibly adopt various conformations regarding the orientation of [Pt(PR$_3$)$_2$(C)$_2$] and arylene units.[28] In the present study, we checked the relationship between the relative energy and dihedral angle φ defined by C$^{\alpha}$–C$^{\beta}$–Pt–P$^{\alpha}$ (Fig. 10) from 0° to 90° at 10 degree increments for the model of monomer unit of poly(***p,p*-1-2c**). The conformer with φ = 90° was energetically most stable, and the energy gradually increased with decreasing φ. The energy difference between the most stable (φ = 90°) and most unstable (φ = 10°) conformers was 3.75 kJ/mol. It is likely that the conformations are interchangeable with rotations around Pt moieties due to the small rotational barrier as reported for several Pt-acetylide oligomers.[28] We then simulated the aggregation of four model molecules with the most stable conformer (φ = 90°). In the starting geometries of the aggregates of model molecules, dummy atoms (X) were placed at the center of the anthracene moieties (Fig. 11). The model molecules were separated by 3.8 Å at the dummy atoms, and then rotated by 30°, 45°, 60° and 75° (torsional angle at X–X) to avoid overlap between PBu$_3$ groups. In this calculation, M06-2X functional was employed because it is superior compared with the commonly used B3LYP functional in estimating noncovalent interactions including π-stacking.[22] The model with the torsional angle X–X starting from 60° was most stable (Table S1), presumably because the combined stabilization effect by π-stacking of the anthracene rings and van der Waals interactions between the butyl groups was maximum among the four models examined. The stabilization energy was calculated to be 103.97 kJ/mol in the case of a model with the torsional angle X–X starting from 60°. Fig. 12 depicts a structure of the model for aggregation of poly(***p,p*-1-2c**), whose geometries were fully optimized by the M06-2X/6-31G* (C, H, P)-LANL2DZ (Pt). It is likely that this kind of aggregation also occurs between the polymer molecules.

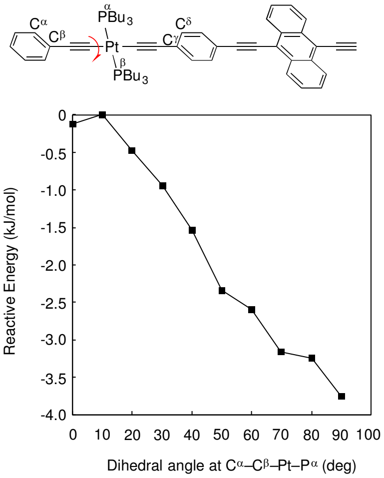

Fig. 10 Relationship between the dihedral angle at C$^{\alpha}$–C$^{\beta}$–Pt–P$^{\alpha}$and relative energy for the model of monomer unit of poly(***p,p*-1-2c**) calculated by the DFT method [B3LYP/6-31G* (C, H, P)-LANL2DZ (Pt)], wherein the bond angle at P$^{\alpha}$–Pt–P$^{\beta}$ was constrained to 180°, and the dihedral angle C$^{\alpha}$–C$^{\beta}$–C$^{\gamma}$–C$^{\delta}$ was constrained to 0°.

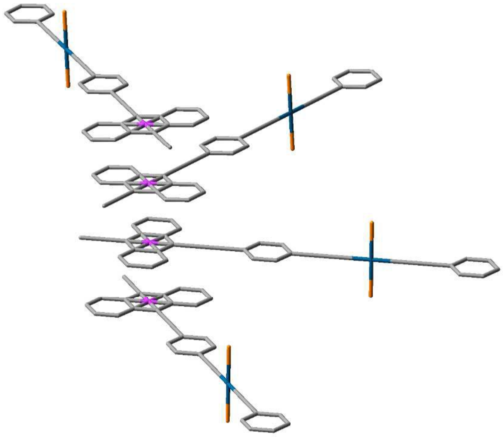

Fig. 11 Model molecules for aggregation. Butyl groups at the phosphine atoms, and all hydrogen atoms are omitted for clarity. Dummy atoms X are indicated in violet. The torsional angle at X–X is 60° in this case.

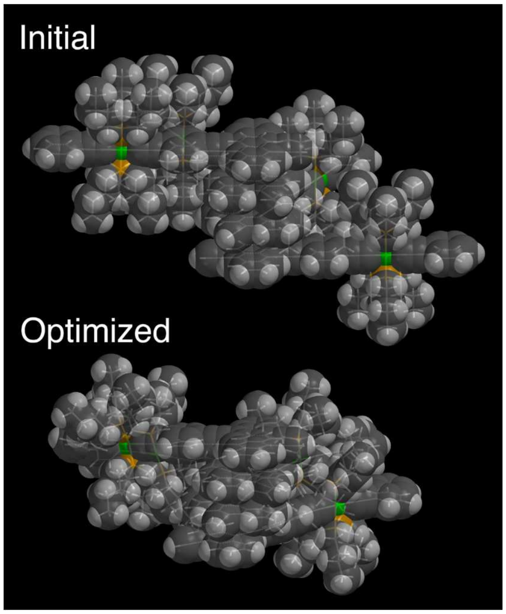

Fig. 12 Initial and optimized possible aggregated structure of model compounds of poly(***p*,*p***-**1**-**2c**). The torsional angle X–X of the initial geometry was set to be 60°, wherein X is a dummy atom placed at the center of anthracene (see Fig. 11). Geometries were optimized by the DFT method [M06-2X/6-31G* (C, H, P)-LANL2DZ (Pt)].

Conclusions

The present paper demonstrated the synthesis of Pt-containing poly(phenyleneethynylene aryleneethynylene)s poly(***m*,*m***-**1**-**2a**)–poly(***p*,*p***-**1**-**2c**) by the Sonogashira-Hagihara coupling polymerization of the Pt-containing diethynyl monomers ***m*,*m*-1** and ***p*,*p*-1** with dibromoarylene monomers **1a**–**1c** using Pd–Cu catalyst. The wavelength maxima of absorption and emission signals of *m*-phenyleneethynylene-linked polymers were shorter than those of the *p*-phenyleneethynylene-linked counterparts. The order of wavelength maxima of λ_{abs} and λ_{emi} of the polymers is as follows, Ar = 1,4-phenylene < 1,4-naphthalene < 9,10-anthracene both for the *m,m*- and *p,p*-linked polymers, apparently reflecting the conjugation length of the arylene chromophores of the polymers. The fluorescence was remarkably influenced by solvent. Representatively, poly(***p*,*p***-**1**-**2c**) formed aggregates in THF/MeOH upon raising MeOH content, resulting in a red-shift of the fluorescence wavelength and decrease of emission intensity. DFT simulations suggested that the driving forces for aggregation are π-stacking between the anthracene units and van der Waals interactions between the phosphine alkyl groups.

Acknowledgements

This research was financially supported by the Kansai University Grant-in-Aid for progress of research in graduate course, 2014–2015, and by a Grant-in-Aid for Scientific Research on Innovative Areas "New Polymeric Materials Based on Element- Blocks (No. 2401)" from the Ministry of Education, Culture, Sports, Science, and Technology, Japan. The authors are grateful to Prof. Yutaka Nishiyama and Prof. Rui Umeda for measurement of absolute fluorescence quantum yields, Dr. Kimihiro Matsukawa and Dr. Motohiro Shizuma for measurement of mass spectra at Osaka Municipal Technical Research Institute, and Prof. Kenneth B. Wagener and Dr. Kathryn R. Williams at the University of Florida for their helpful suggestions and comments.

Notes and references

1 K. Müllen, J. R. Reynolds, T. Masuda, Eds. Conjugated Polymers: A Practical Guide to Synthesis, *RSC Publishing* (Cambridge, UK), 2013.

2 Review: H. Jiang, P. Taranekar, J. R. Reynolds, K. S. Schanze, *Angew. Chem. Int. Ed,* 2009, **48**, 4300–4316.

3 Review: (a) P. M. Beaujuge, C. M. Amb, J. R. Reynolds, *Acc. Chem. Res*, 2010, **43**, 1396–1407. (b) W.-Y. Wong, X.-Z. Wang, Z. He, A. B. Djurisic, C.-T. Yip, K.-Y. Cheung, H. Wang, C. S. K. Mak, W.-K. Chan, Nature Mat., 2007, **6**, 521–527. (c) W.-Y. Wong, X.-Z. Wang, Z. He, K.-K. Chan, A. B. Djurisic, K.-Y. Cheung, C.-T. Yip, A. M.-C. Ng, Y. Y. Xi, C. S. K. Mak, W.-K. Chan, *J. Am. Chem. Soc.* 2007, **129**, 14372–14380. (d) L. Liu, C.-L. Ho, W.-Y. Wong, K.-Y. Cheung, M.-K. Fung, W.-T. Lam, A. B. Djurisic, W.-K. Chan, *Adv. Funct. Mater.* 2008, **18**, 2824–2833. (e) W.-Y. Wong, C.-L. Ho, *Acc. Chem. Res.* 2010, **43**, 1246–1256. (f) W.-Y. Wong, *Macromol. Chem. Phys.* 2008, **209**, 14–24.

4 Reviews: (a) X. Chen, G. Zhou, X. Peng, J. Yoon, *Chem. Soc. Rev.* 2012, **41**, 4610–4630. (b) S. Rochat, T. M. Swager, *ACS Appl. Mater. Interfaces* 2013, **5**, 4488–4502.

5 Reviews: (a) U. H. F. Bunz, *Acc. Chem. Res.* 2001**, 34**, 998–1010. (b) D. J. Hill, M. J. Mio, R. B. Prince, T. S. Hughes, J. S. Moore, *Chem. Rev.* 2001, **101**, 3893–4011. (c) W. Zhang, J. S. Moore, *Angew. Chem. Int. Ed.* 2006, **45**, 4416–4439. (d) L. Zang, Y. Che, J. S. Moore, *Acc. Chem. Res.* 2008, **41**, 1596–1608. (e) Y. Wang, E. Y. Chi, K. S. Schanze, D. G. Whitten, *Soft Matter* 2012, **8**, 8547–8558. (f) R. Hu, J. W. Y. Lam, B. Z. Tang, *Macromol. Chem. Phys.* 2013, **214**, 175–187.

6 (a) Y. Fujikura, K. Sonogashira, N. Hagihara, *Chem. Lett*. 1975, **10**, 1067–1070. (b) K. Sonogashira, S. Takahashi, N. Hgihara, *Macromolecules*, 1977, **10**, 879–880. (c) K. Sonogashira, S. Kataoka, S. Takahashi, N. Hagihara, *J. Organomet. Chem*. 1978, **160**, 319–327. (d) S. Takahashi, M. Kariya, T. Yatake, K. Sonogashira, N. Hagihara, *Macromolecules* 1978, **11**, 1063–1066.

7 (a) M.–H. Nguyen, J. H. K. Yip, *Organometallics*, 2012, **31**, 7522–7531. (b) J. M. Keller, K. D. Glusac, E. O. Danilov, S. Mcilroy, P. Sreearuothai, A. R. Cook, H. Jiang, J. R. Miller, K. S. Schanze, *J. Am. Chem. Soc.* 2011, **133**, 11289–11298. (c) W.-Y. Wong, C.-L. Ho, *Coord. Chem. Rev*, 2006, **250**, 2627–2690. (d) W.-Y. Wong, Dalton Trans., 2007, 4495–4510. (e) C.-L. Ho, W.-Y. Wong, *Coord. Chem. Rev*, 2011, **255**, 2469–2502. (f) W.-Y. Wong, P. D. Harvey, *Macromol. Rapid Commun.* 2010, **31**, 671–713. (g) C.-L. Ho, W.-Y. Wong, *Coord. Chem. Rev*, 2013, **257**, 1614–1649. (h) W.-Y. Wong, *J. Inorg. Organomet. Polym. Mater.* 2005, **15**, 197–219.

8 (a) E. E. Silverman, T. Cardolaccia, X. Zhao, K.–Y. Kim, K. H. Glusac, K. S. Schanze, *Coord. Chem. Rev.* 2005, **249**, 1491–1500. (b) T. Cardolaccia, Y. Li, K. S. Schanze, *J. Am. Chem. Soc.* 2008, **130**, 2535–2545. (c) F. Guo, Y. G.

Kim, J. R. Reynolds, K. S. Schanze, *Chem. Commun.* 2006, **17**, 1887–1889. (d) C. Liao, A. H. Shelton, K.–Y. Kim, K. S. Schanze, *ACS Appl. Mater. Interfaces* 2011, **3**, 3225–3238. (e) C. Liao, A. H. Shelton, K.–Y. Kim, K. S. Schanze, *ACS Appl. Mater. Interfaces* 2011, **3**, 3225–3238. (f) Y. Li, M. E. Köse, K. S. Schanze, *J. Phys. Chem. B* 2013, **117**, 9025−9033. (g) W.-Y. Wong, G.-L. Lu, K.-H. Choi, J.-X. Shi, *Macromolecules* 2002, **35**, 3506–3513. (h) W.-Y. Wong, L. Liu, S.-Y. Poon, K.-H. Choi, K.-W. Chesh, J.-X. Shi, *Macromolecules* 2004, **37**, 4496–4504. (i) S. M. Aly, C.-L. Ho, W.-Y. Wong, D. Fortin, P. D. Harvey, *Macromolecules* 2009, **42**, 6902–6916.

9 Reviews: (a) S.-K. Choi, Y.-S. Gal, S.-H. Jin and H. K. Kim, *Chem. Rev.*, 2000, **100**, 1645–1681. (b) T. Aoki, T. Kaneko and M. Teraguchi, *Polymer*, 2006, **47**, 4867–4892. (c) T. Masuda, *J. Polym. Sci., Part A: Polym. Chem.*, 2007, **45**, 165–180. (d) T. Masuda, F. Sanda, M. Shiotsuki, Polymerization of Acetylenes, in Comprehensive Organometallic Chemistry III, ed. R. Crabtree and M. Mingos, Elsevier, Oxford, 2007, vol. 11, ch. 16, pp. 557–593. (e) E. Yashima, K. Maeda, H. Iida, Y. Furusho, K. Nagai, *Chem. Rev.*, 2009, **109**, 6102–6211; (f) K. Akagi, *Chem. Rev.*, 2009, **109**, 5354–5401. (g) J. Liu, J. W. Y. Lam, B. Z. Tang, *Chem. Rev.*, 2009, **109**, 5799–5867. (h) T. Masuda, M. Shiotsuki, F. Sanda, Product Class 31: Macromolecular Conjugated Polyenes, in Science of Synthesis. Houben-Weyl Methods of Molecular Transformations, Category 6, ed. J. S. Siegel and Y. Tobe, Georg Thieme Verlag KG, Stuttgart, New York, 2010, vol. 45b, pp. 1421–1439. (i) M. Shiotsuki, F. Sanda, T. Masuda, *Polym. Chem.*, 2011, **2**, 1044–1058.

10 C. F. J. Faul, *Acc. Chem. Res.* 2014, **47**, 3428−3438.

11 Reviews: (a) D. Türp, T.-T.-T. Nguyen, M. Baumgarten, K. Müllen, *New J. Chem.*, 2012, **36**, 282–298. (b) B. Schmaltz, T. Weil, K. Müllen, *Adv. Mater.* 2009, **21**, 1067–1078.

12 Reviews: (a) V. Savvateev, A. Yakimov, D. Davidov, *Adv. Mater.* 1999, **11**, 519–531. (b) G. Hughes, M. R. Bryce, *J. Mater. Chem.* 2005, **15**, 94–107. (c) A. Ajayaghosh, V. K. Praveen, *Acc. Chem. Res.* 2007, **40**, 644–656. (d) J. C. García-Martínez, E. Díez-Barra, J. Rodríguez-López, *Curr. Org. Syn.* 2008, **5**, 267–290.

13 Reviews: (a) U. H. F. Bunz, *Macromol. Rapid Commun.* 2009, **30**, 772–805. (b) R. A. Smaldone, J. S. Moore, *Chem. Eur. J.* 2008, **14**, 2650–2657. (c) U. H. F. Bunz, *Adv. Polym. Sci.* 2005, **177**, 1–52.

14 Wong et al. have reported Hg polyyne aggregation effects. See (a) W.-Y. Wong, *Coord. Chem. Rev.* 2007, **251**, 2400–2427. (b) W.-Y. Wong, L. Liu, J.-X. Shi, *Angew. Chem. Int. Ed.* 2003, **42**, 4064–4068. (c) L. Liu, W.-H. Ai, M.-J. Li, S.-Z. Liu, C.-M. Zhang, H.-X. Yan, Z.-L. Du, W.-Y. Wong, *Chem. Mater.*, 2007, **19**, 1704–1711. (d) L. Liu, W.-Y. Wong, J.-X. Shi, K.-W. Cheah, *J. Polym. Sci. A: Polym. Chem.* 2006, **44**, 5588–5607. (e) W.-Y. Wong, K.-H. Choi, G.-L. Lu, Z. Lin, *Organometallics*, 2002, **21**, 4475–4481.

15 (a) R. Liu, F. Sanda, T. Masuda, *J. Polym. Sci., Part A: Polym. Chem.* 2008, **46**, 4183-4192. (b) R. Liu, M. Shiotsuki, T. Masuda, F. Sanda, *Macromolecules* 2009, **42**, 6115–6122. (c) R. Liu, H. Sogawa, M. Shiotsuki, T. Masuda, F. Sanda, *Polymer* 2010, **51**, 2255–2263. (d) H. Sogawa, M. Shiotsuki, H. Matsuoka, F. Sanda, *Macromolecules* 2011, **44**, 3338–3345. (e) T. Ueda, M. Shiotsuki, F. Sanda, *Polymer* 2011, **52**, 3570–3579. (f) A. Hashimoto, H. Sogawa, M. Shiotsuki, F. Sanda, *Polymer* 2012, **53**, 2559–2566. (g) H. Sogawa, M. Shiotsuki, F. Sanda, *Macromolecules* 2013, **46**, 4378–4387. (h) H. Sogawa, M. Shiotsuki, T. Hirao, T. Haino, F. Sanda, *Macromolecules* 2013, **46**, 8161–8170. (i) H. Sogawa, Y. Miyagi, M. Shiotsuki, F. Sanda, *Macromolecules* 2013, **46**, 8896–8904. (j) A. Hashimoto, Y. Miyagi, H. Sogawa, S. Yamamoto, F. Sanda, *Chem. Lett.* 2014, **43**, 1622–1624. (k) Y. Miyagi, H. Sogawa, M. Shiotsuki, F. Sanda, *Macromolecules* 2014, **47**, 1594–1603. (l) Y. Otaki, Y. Miyagi, F. Sanda, *Chem. Lett.* 2015, **44**, 1013–1015.

16 Y. Miyagi, T. Hirao, T. Haino, F. Sanda, *J. Polym. Sci., Part A: Polym. Chem*. 2015, **53**, 2452–2461.

17 Y. Liu, S. Jiang, K. Glusac, D. H. Powell, D. F. Anderson, K. S. Schanze, *J. Am. Chem. Soc.* 2002, **124**, 12412–12413.

18 N. Miyaura, A. Suzuki, *Org. Synth.* 1993, **8**, 532–534.

19 J. A. Rahn, L. Baltusis, J. H. Nelson, *Inorg. Chem.* 1990, **29**, 750–755.

20 M. J. Frisch, G. W. Trucks, H. B. Schlegel, G. E. Scuseria, M. A. Robb, J. R. Cheeseman, G. Scalmani, V. Barone, B. Mennucci, G. A. Petersson, H. Nakatsuji, M. Caricato, X. Li, H. P. Hratchian, A. F. Izmaylov, J. Bloino, G. Zheng, J. L. Sonnenberg, M. Hada, M. Ehara, K. Toyota, R. Fukuda, J. Hasegawa, M. Ishida, T. Nakajima, Y. Honda, O. Kitao, H. Nakai, T. Vreven, J. A. Montgomery, Jr., J. E. Peralta, F. Ogliaro, M. Bearpark, J. J. Heyd, E. Brothers, K. N. Kudin, V. N. Staroverov, T. Keith, R. Kobayashi, J. Normand, K. Raghavachari, A. Rendell, J. C. Burant, S. S. Iyengar, J. Tomasi, M. Cossi, N. Rega, J. M. Millam, M. Klene, J. E. Knox, J. B. Cross, V. Bakken, C. Adamo, J. Jaramillo, R. Gomperts, R. E. Stratmann, O. Yazyev, A. J. Austin, R. Cammi, C. Pomelli, J. W. Ochterski, R. L. Martin, K. Morokuma, V. G. Zakrzewski, G. A. Voth, P. Salvador, J. J. Dannenberg, S. Dapprich, A. D. Daniels, O. Farkas, J. B. Foresman, J. V. Ortiz, J. Cioslowski, D. J. Fox, Gaussian, Inc., Wallingford CT, 2013.

21 R. G. Parr, W. Yang, Density-Functional Theory of Atoms and Molecules; Oxford University Press (Oxford, UK), 1989.

22 Y. Zhao, D. G. Truhlar, *Theor. Chem. Acc.*, 2008, **120**, 215–241.

23 Data measured in EtOH.

24 We compared the band gaps of the model compounds for the polymers with and without Pt. The band gaps of the *m*-linked models with Pt tend to be narrower than those of the models without Pt. We measured the cyclic votammetry of the polymers but failed to obtain clear data. If we could determine the band gaps of the polymers directly, we would provide more detailed information on the electric properties. Further analysis is under investigation.

25 The differences of band edges between the polymers were negligibly small (Fig. S2).

26 (a) G. R. Suman, S. G. Bubbly, S. B. Gudennavar, J. Thipperudrappa, B. Roopashree, V. Gayathri, N. M. Nanja Gowda, *Luminescence*, 2015, **30**, 611–618. (b) D. Nagaraja, R. M. Melavanki, N. R. Patil, H. S. Geethanjali, R. A. Kusanur, *Luminescence*, 2015, **30**, 495–502.

27 No particle was observed at 0–30% MeOH contents. When MeOH content exceeded 40%, the polymer formed 200–400 nm particles irrespective of MeOH content.

28 (a) K. Haskins-Glusac, I. Ghiviriga, K. A. Abboud, K. S. Schanze, *J. Phys. Chem. B* 2004, **108**, 4969–4978. (b) K. Glusac, M. E. Köse, J. Jiang, K. S. Schanze, *J. Phys. Chem. B* 2007, **111**, 929–940.

Graphical Abstract

Various platinum-containing phenylene-ethynylene-arylene polymers were synthesized, and the relationships between the optical properties and aggregation behaviour were examined .